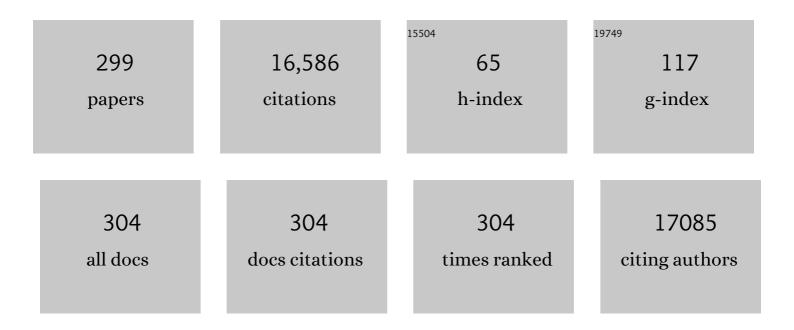
List of Publications by Year in descending order

Source: https://exaly.com/author-pdf/6297090/publications.pdf Version: 2024-02-01



MENCTAO SUN

#	Article	IF	CITATIONS
1	Graphene-based SERS for sensor and catalysis. Applied Spectroscopy Reviews, 2023, 58, 1-38.	6.7	39
2	Molecular and plasmonic resonances on tip-enhanced Raman spectroscopy. Spectrochimica Acta - Part A: Molecular and Biomolecular Spectroscopy, 2022, 265, 120360.	3.9	3
3	In situ Plasmon-Enhanced CARS and TPEF for Gram staining identification of non-fluorescent bacteria. Spectrochimica Acta - Part A: Molecular and Biomolecular Spectroscopy, 2022, 264, 120283.	3.9	27
4	Tip-enhanced two-photon-excited fluorescence of monolayer MoS2. Applied Surface Science, 2022, 576, 151835.	6.1	5
5	Phonon-assisted Interfacial Charge Transfer Excitons in Graphene/h-BN van der Waals Heterostructures. Chinese Journal of Physics, 2022, 76, 110-120.	3.9	2
6	Nanoscale engineering of ring-mounted nanostructure around AAO nanopores for highly sensitive and reliable SERS substrates. Nanotechnology, 2022, 33, 135501.	2.6	9
7	Two-Dimensional Self-Assembly of Au@Ag Core–Shell Nanocubes with Different Permutations for Ultrasensitive SERS Measurements. ACS Omega, 2022, 7, 3312-3323.	3.5	14
8	Optical non-reciprocity with multiple modes in the visible range based on a hybrid metallic nanowaveguide. Journal Physics D: Applied Physics, 2022, 55, 195102.	2.8	0
9	Electronic structures and optical properties of monolayer borophenes. Spectrochimica Acta - Part A: Molecular and Biomolecular Spectroscopy, 2022, 272, 121014.	3.9	6
10	Unified treatment for photoluminescence and scattering of coupled metallic nanostructures: I. Two-body system. New Journal of Physics, 2022, 24, 033026.	2.9	8
11	Bilayer borophene synthesized on Ag(111) film: Physical mechanism and applications for optical sensor and thermoelectric devices. Materials Today Physics, 2022, 23, 100652.	6.0	15
12	Nonlinear Optical Microscopy and Plasmon Enhancement. Nanomaterials, 2022, 12, 1273.	4.1	5
13	Tip-enhanced Raman spectroscopy. Reviews in Physics, 2022, 8, 100067.	8.9	34
14	Strongly enhanced propagation and non-reciprocal properties of CdSe nanowire based on hybrid nanostructures at communication wavelength of 1550 nm. Optics Communications, 2022, 514, 128175.	2.1	1
15	Exploring Nonemissive Excited-State Intramolecular Proton Transfer by Plasmon-Enhanced Hyper-Raman Scattering and Two-Photon Excitation Fluorescence. Journal of Physical Chemistry C, 2022, 126, 487-492.	3.1	22
16	Nonlinear plexcitons: excitons coupled with plasmons in two-photon absorption. Nanoscale, 2022, 14, 7269-7279.	5.6	27
17	Transition Metal Dichalcogenides (TMDCs) Heterostructures: Synthesis, Excitons and Photoelectric Properties. Chemical Record, 2022, 22, e202100313.	5.8	12
18	Polarization and incident angle-dependent plasmonic coupling of Au@Ag nanoalloys. Chinese Journal of Physics, 2022, 78, 132-140.	3.9	7

#	Article	IF	CITATIONS
19	Spectral investigation on single molecular optoelectronics of ladder phenylenes. Spectrochimica Acta - Part A: Molecular and Biomolecular Spectroscopy, 2022, 278, 121283.	3.9	3
20	Unified treatment for photoluminescence and scattering of coupled metallic multi–nanostructures. Results in Physics, 2022, , 105668.	4.1	0
21	Perspective on plexciton based on transition metal dichalcogenides. Applied Physics Letters, 2022, 120, .	3.3	23
22	Transition metal dichalcogenides (TMDCs) heterostructures: Optoelectric properties. Frontiers of Physics, 2022, 17, .	5.0	25
23	Nonlinear optical microscopies: physical principle and applications. Applied Spectroscopy Reviews, 2021, 56, 52-66.	6.7	9
24	Electronic circular dichroism and Raman optical activity: Principle and applications. Applied Spectroscopy Reviews, 2021, 56, 553-587.	6.7	18
25	Chiral surface plasmon-enhanced chiral spectroscopy: principles and applications. Nanoscale, 2021, 13, 581-601.	5.6	43
26	Physical mechanism and electric-magnetic interaction in ECD and ROA: Visualization methods on chirality. Chemical Physics Letters, 2021, 763, 138206.	2.6	1
27	Two-dimensional WS ₂ /MoS ₂ heterostructures: properties and applications. Nanoscale, 2021, 13, 5594-5619.	5.6	73
28	High-performance SERS substrate based on perovskite quantum dot–graphene/nano-Au composites for ultrasensitive detection of rhodamine 6G and <i>p</i> -nitrophenol. Journal of Materials Chemistry C, 2021, 9, 9011-9020.	5.5	18
29	Plexcitons, electric field gradient and electron–phonon coupling in tip-enhanced Raman spectroscopy (TERS). Nanoscale, 2021, 13, 10712-10725.	5.6	14
30	Plasmon and Plexciton Driven Interfacial Catalytic Reactions. Chemical Record, 2021, 21, 797-819.	5.8	49
31	Electromagnetic Field Gradient-Enhanced Raman Scattering in TERS Configurations. Journal of Physical Chemistry C, 2021, 125, 5684-5691.	3.1	10
32	Molecular chirality of Macrolide antibiotics. Chemical Physics, 2021, 545, 111120.	1.9	0
33	Pressure-dependent interfacial charge transfer excitons in WSe2-MoSe2 heterostructures in near infrared region. Results in Physics, 2021, 24, 104110.	4.1	22
34	Graphene plasmon for optoelectronics. Reviews in Physics, 2021, 6, 100054.	8.9	54
35	Plexciton and electron–phonon interaction in tipâ€enhanced resonance Raman scattering. Journal of Raman Spectroscopy, 2021, 52, 1685.	2.5	5
36	Engineering plasmonic nanochain for optical sensor via regulating electric field. Optik, 2021, 240, 166827.	2.9	4

#	Article	IF	CITATIONS
37	Photoinduced charge transfer in two-photon absorption. Results in Optics, 2021, 4, 100099.	2.0	2
38	Plexciton in tip-enhanced resonance Stokes and anti-Stokes Raman spectroscopy and in propagating surface plasmon polaritons. Optics Communications, 2021, 493, 126990.	2.1	13
39	Physical Mechanisms on Plasmon-Enhanced Organic Solar Cells. Journal of Physical Chemistry C, 2021, 125, 21301-21309.	3.1	36
40	Structural Color Control of CoFeB-Coated Nanoporous Thin Films. Coatings, 2021, 11, 1123.	2.6	7
41	External electric field manipulating sequential and super-exchange charge transfer in donor-bridge-acceptor system in two-photon absorption. Physica E: Low-Dimensional Systems and Nanostructures, 2021, 134, 114840.	2.7	14
42	Unified treatments for localized surface plasmon resonance and propagating surface plasmon polariton based on resonance modes in metal nanowire. Optics Communications, 2021, 499, 127277.	2.1	21
43	Aluminum plasmon-enhanced deep ultraviolet fluorescence resonance energy transfer in h-BN/graphene heterostructure. Optics Communications, 2021, 498, 127224.	2.1	11
44	Graphene Plasmon-Enhanced Polarization-Dependent Interfacial Charge Transfer Excitons in 2D Graphene-Black Phosphorus Heterostructures in NIR and MIR Regions. Journal of Physical Chemistry C, 2021, 125, 22370-22378.	3.1	14
45	Plasmonic alloy nanochains assembled via dielectrophoresis for ultrasensitive SERS. Optics Express, 2021, 29, 36857.	3.4	8
46	Physical mechanisms of photoinduced charge transfer in neutral and charged donor–acceptor systems. RSC Advances, 2021, 11, 38302-38306.	3.6	1
47	Carbon Dots: Synthesis, Properties and Applications. Nanomaterials, 2021, 11, 3419.	4.1	115
48	Flexible and transparent Au nanoparticle/graphene/Au nanoparticle â€~sandwich' substrate for surface-enhanced Raman scattering. Materials Today Nano, 2020, 9, 100067.	4.6	28
49	External Electric Field-Dependent Photoinduced Charge Transfer in a Donor–Acceptor System in Two-Photon Absorption. Journal of Physical Chemistry C, 2020, 124, 2319-2332.	3.1	38
50	Voltage-manipulating graphene-mediated surface-enhanced Raman scattering (G-SERS): principle and applications. Applied Spectroscopy Reviews, 2020, 55, 558-573.	6.7	9
51	Plexciton for surface enhanced Raman scattering and emission. Journal of Raman Spectroscopy, 2020, 51, 476-482.	2.5	8
52	Photoninduced charge redistribution of graphene determined by edge structures in the infrared region. Spectrochimica Acta - Part A: Molecular and Biomolecular Spectroscopy, 2020, 229, 117858.	3.9	8
53	Photo-physical properties of vinigrol revealed by two-photon absorption, electronic circular dichroism, Raman spectroscopy and Raman optical activity. Chemical Physics Letters, 2020, 755, 137798.	2.6	4
54	Optical physics on chiral brominated azapirones: Bromophilone A and B. Spectrochimica Acta - Part A: Molecular and Biomolecular Spectroscopy, 2020, 242, 118780.	3.9	5

#	Article	IF	CITATIONS
55	Optical properties of kalihinol derivatives in TPA, ECD and ROA. Chemical Physics Letters, 2020, 755, 137796.	2.6	3
56	Graphitic carbon nitride-based 2D catalysts for green energy: Physical mechanism and applications. Materials Today Energy, 2020, 17, 100488.	4.7	14
57	Nanoplasmonic Nanorods/Nanowires from Single to Assembly: Syntheses, Physical Mechanisms and Applications. Chemical Record, 2020, 20, 1043-1073.	5.8	4
58	Electrochemical synthesis of tin plasmonic dendritic nanostructures with SEF capability through <i>in situ</i> replacement. RSC Advances, 2020, 10, 36042-36050.	3.6	5
59	Interfacial charge transfer exciton enhanced by plasmon in 2D in-plane lateral and van der Waals heterostructures. Applied Physics Letters, 2020, 117, .	3.3	85
60	Functionalized Gold Nanoparticles: Synthesis, Properties and Biomedical Applications. Chemical Record, 2020, 20, 1474-1504.	5.8	91
61	Photoinduced charge transfer in quasi-one-dimensional polymers in two-photon absorption. RSC Advances, 2020, 10, 33288-33298.	3.6	3
62	Mechanical properties of Fe-based bulk amorphous Fe41Co7Cr15Mo14C15B6Y2 alloy rods. Chemical Physics Letters, 2020, 750, 137511.	2.6	10
63	Plasmonic Nanoparticle Film for Low-Power NIR-Enhanced Photocatalytic Reaction. ACS Applied Materials & Interfaces, 2020, 12, 16753-16761.	8.0	12
64	Synthesis of homogeneous carbon quantum dots by ultrafast dual-beam pulsed laser ablation for bioimaging. Materials Today Nano, 2020, 12, 100091.	4.6	66
65	Photoinduced Charge Transfer in Donor-Bridge-Acceptor in One- and Two-photon Absorption: Sequential and Superexchange Mechanisms. Journal of Physical Chemistry C, 2020, 124, 4968-4981.	3.1	39
66	Optoelectronic and photoelectric properties and applications of graphene-based nanostructures. Materials Today Physics, 2020, 13, 100196.	6.0	42
67	Spectral analysis on CoOx films deposited by atomic layer deposition. Chemical Physics Letters, 2020, 742, 137159.	2.6	2
68	One―and Twoâ€Photon Absorption: Physical Principle and Applications. Chemical Record, 2020, 20, 894-911.	5.8	7
69	The linear and non-linear optical absorption and asymmetrical electromagnetic interaction in chiral twisted bilayer graphene with hybrid edges. Materials Today Physics, 2020, 14, 100222.	6.0	52
70	Nonlinear optical microscopies (NOMs) and plasmon-enhanced NOMs for biology and 2D materials. Nanophotonics, 2020, 9, 1341-1358.	6.0	6
71	Graphitic carbon nitride nanostructures: Catalysis. Applied Materials Today, 2019, 16, 388-424.	4.3	58
72	Visualizations of Electric and Magnetic Interactions in Electronic Circular Dichroism and Raman Optical Activity. Journal of Physical Chemistry A, 2019, 123, 8071-8081.	2.5	43

#	Article	IF	CITATIONS
73	Nanoscale Vertical Arrays of Gold Nanorods by Self-Assembly: Physical Mechanism and Application. Nanoscale Research Letters, 2019, 14, 118.	5.7	40
74	Tuning the SERS activity and plasmon-driven reduction of <i>p</i> -nitrothiophenol on a Ag@MoS ₂ film. Faraday Discussions, 2019, 214, 297-307.	3.2	26
75	Properties and applications of new superlattice: twisted bilayer graphene. Materials Today Physics, 2019, 9, 100099.	6.0	62
76	Tunable electron transfer rate in a CdSe/ZnS-based complex with different anthraquinone chloride substitutes. Scientific Reports, 2019, 9, 7756.	3.3	5
77	Visualization of Photoinduced Charge Transfer and Electron–Hole Coherence in Two-Photon Absorption. Journal of Physical Chemistry C, 2019, 123, 14132-14143.	3.1	81
78	Porous size dependent g-C3N4 for efficient photocatalysts: Regulation synthesizes and physical mechanism. Materials Today Energy, 2019, 13, 11-21.	4.7	41
79	Tipâ€enhanced spectroscopy of 2D black phosphorus. Journal of Raman Spectroscopy, 2019, 50, 1058-1064.	2.5	13
80	Biological nascent evolution of snail bone and collagen revealed by nonlinear optical microscopy. Journal of Biophotonics, 2019, 12, e201900119.	2.3	12
81	Optoelectronic properties and applications of graphene-based hybrid nanomaterials and van der Waals heterostructures. Applied Materials Today, 2019, 16, 1-20.	4.3	82
82	Transformation from Quantum to Classical Mode: the Size Effect of Plasmon in 2D Atomic Cluster System. Scientific Reports, 2019, 9, 6641.	3.3	1
83	Optical-electrical synergy on electricity manipulating plasmon-driven photoelectrical catalysis. Applied Materials Today, 2019, 15, 305-314.	4.3	10
84	Excitonâ^'Plasmon Interactions in Noble Metal–Semiconductor Oxide Hybrid Nanostructures. , 2019, , 157-178.		0
85	Multiple surface plasmon resonances enhanced nonlinear optical microscopy. Nanophotonics, 2019, 8, 487-493.	6.0	41
86	Two-dimensional black phosphorus: physical properties and applications. Materials Today Physics, 2019, 8, 92-111.	6.0	68
87	Physical mechanism on edge-dependent electrons transfer in graphene in mid infrared region. Spectrochimica Acta - Part A: Molecular and Biomolecular Spectroscopy, 2019, 216, 136-145.	3.9	7
88	Plasmon-driven molecular photodissociations. Applied Materials Today, 2019, 15, 212-235.	4.3	13
89	Plasmonâ€Enhanced Fluorescence Resonance Energy Transfer. Chemical Record, 2019, 19, 818-842.	5.8	41
90	The Thermal, Electrical and Thermoelectric Properties of Graphene Nanomaterials. Nanomaterials, 2019, 9, 218.	4.1	52

#	Article	IF	CITATIONS
91	Nonlinear optical characterization of porous carbon materials by CARS, SHG and TPEF. Spectrochimica Acta - Part A: Molecular and Biomolecular Spectroscopy, 2019, 214, 58-66.	3.9	11
92	Plasmonic nanoparticle-film-assisted photoelectrochemical catalysis across the entire visible-NIR region. Nanoscale, 2019, 11, 23058-23064.	5.6	10
93	Plasmon-exciton coupling by hybrids between graphene and gold nanorods vertical array for sensor. Applied Materials Today, 2019, 14, 166-174.	4.3	69
94	Deep ultraviolet tip-enhanced fluorescence. Nanotechnology, 2019, 30, 035202.	2.6	2
95	The nature of photoinduced intermolecular charger transfer in fluorescence resonance energy transfer. Spectrochimica Acta - Part A: Molecular and Biomolecular Spectroscopy, 2019, 209, 228-233.	3.9	19
96	Physical principle and advances in plasmon-enhanced upconversion luminescence. Applied Materials Today, 2019, 15, 43-57.	4.3	40
97	The nature of chirality induced by molecular aggregation and self-assembly. Spectrochimica Acta - Part A: Molecular and Biomolecular Spectroscopy, 2019, 212, 188-198.	3.9	26
98	Study of Surface Plasmon Assisted Reactions to Understand the Light-Induced Decarboxylation of N719 Sensitizer. European Journal of Inorganic Chemistry, 2019, 2019, 23-28.	2.0	6
99	The Remote Light Emission Modulated by Local Surface Plasmon Resonance for the CdSe NW–Au NP Hybrid Structure. Advanced Materials Interfaces, 2019, 6, 1801418.	3.7	4
100	Plasmon-enhanced upconversion photoluminescence: Mechanism and application. Reviews in Physics, 2019, 4, 100026.	8.9	105
101	Ultrafast carrier dynamics in all-inorganic CsPbBr ₃ perovskite across the pressure-induced phase transition. Optics Express, 2019, 27, A995.	3.4	29
102	Surface catalytic reaction driven by plasmonic waveguide. Applied Materials Today, 2018, 11, 50-56.	4.3	7
103	Electro-optical tuning of plasmon-driven double reduction interface catalysis. Applied Materials Today, 2018, 11, 189-192.	4.3	17
104	Physical mechanism of photoinduced intermolecular charge transfer enhanced by fluorescence resonance energy transfer. Physical Chemistry Chemical Physics, 2018, 20, 13558-13565.	2.8	37
105	Photocatalytic activity of silver oxide capped Ag nanoparticles constructed by air plasma irradiation. Applied Physics Letters, 2018, 112, .	3.3	12
106	Unraveling the Raman Enhancement Mechanism on 1T′â€₱hase ReS ₂ Nanosheets. Small, 2018, 14, e1704079.	10.0	87
107	Electrically enhanced hot hole driven oxidation catalysis at the interface of a plasmon–exciton hybrid. Nanoscale, 2018, 10, 5482-5488.	5.6	110
108	Propagating surface plasmon polaritons for remote excitation surface-enhanced Raman scattering spectroscopy. Applied Spectroscopy Reviews, 2018, 53, 771-782.	6.7	12

#	Article	IF	CITATIONS
109	Charge-transfer channel in quantum dot–graphene hybrid materials. Nanotechnology, 2018, 29, 145202.	2.6	8
110	Femtosecond dynamics of monolayer MoS2-Ag nanoparticles hybrid probed at 532â€ [–] nm. Chemical Physics Letters, 2018, 692, 208-213.	2.6	9
111	Combustion kinetics and structural features of bituminous coal before and after modification process. Journal of Thermal Analysis and Calorimetry, 2018, 131, 983-992.	3.6	12
112	Self-assembly of Au@Ag core–shell nanocuboids into staircase superstructures by droplet evaporation. Nanoscale, 2018, 10, 142-149.	5.6	44
113	Plasmonâ€Exciton Coupling Interaction for Surface Catalytic Reactions. Chemical Record, 2018, 18, 481-490.	5.8	44
114	Exciton-plasmon coupling interactions: from principle to applications. Nanophotonics, 2018, 7, 145-167.	6.0	164
115	The nature of plasmonâ€exciton codriven surface catalytic reaction. Journal of Raman Spectroscopy, 2018, 49, 383-387.	2.5	13
116	Plasmonic electrons enhanced resonance Raman scattering (EERRS) and electrons enhanced fluorescence (EEF) spectra. Applied Materials Today, 2018, 13, 298-302.	4.3	22
117	Influence of the external field on the excitation properties of plasmon in linear atomic chain. Scientific Reports, 2018, 8, 12563.	3.3	2
118	Site-selected N vacancy of g-C3N4 for photocatalysis and physical mechanism. Applied Materials Today, 2018, 13, 329-338.	4.3	66
119	Ag Nanoparticle-Induced Oxidative Dimerization of Thiophenols: Efficiency and Mechanism. Langmuir, 2018, 34, 11347-11353.	3.5	9
120	Magnetic field modulated SERS enhancement of CoPt hollow nanoparticles with sizes below 10 nm. Nanoscale, 2018, 10, 12650-12656.	5.6	14
121	Nanocrystallization and magnetostriction coefficient of Fe52Co34Hf7B6Cu1 amorphous alloy treated by medium-frequency magnetic pulse. Journal of Magnetism and Magnetic Materials, 2018, 468, 181-184.	2.3	7
122	Exciton–plasmon hybrids for surface catalysis detected by SERS. Nanotechnology, 2018, 29, 372001.	2.6	17
123	Physical Insight on Mechanism of Photoinduced Charge Transfer in Multipolar Photoactive Molecules. Scientific Reports, 2018, 8, 10089.	3.3	14
124	Photoinduced charge transfer by one and two-photon absorptions: physical mechanisms and applications. Physical Chemistry Chemical Physics, 2018, 20, 19720-19743.	2.8	27
125	Optical characterizations of two-dimensional materials using nonlinear optical microscopies of CARS, TPEF, and SHG. Nanophotonics, 2018, 7, 873-881.	6.0	35
126	The thermal and thermoelectric properties of in-plane C-BN hybrid structures and graphene/h-BN van der Waals heterostructures. Materials Today Physics, 2018, 5, 29-57.	6.0	79

#	Article	IF	CITATIONS
127	Advances in nonlinear optical microscopy for biophotonics. Journal of Nanophotonics, 2018, 12, 1.	1.0	24
128	Plasmon-Driven Diazo Coupling Reactions of p-Nitroaniline via â^'NH2 or â^'NO2 in Atmosphere Environment. Journal of Physical Chemistry C, 2017, 121, 5225-5231.	3.1	37
129	Screening and design of high-performance indoline-based dyes for DSSCs. RSC Advances, 2017, 7, 20520-20536.	3.6	44
130	Non-symmetric hybrids of noble metal-semiconductor: Interplay of nanoparticles and nanostructures in formation dynamics and plasmonic applications. Progress in Natural Science: Materials International, 2017, 27, 157-168.	4.4	19
131	Morphological effects on the selectivity of intramolecular versus intermolecular catalytic reaction on Au nanoparticles. Nanoscale, 2017, 9, 7727-7733.	5.6	17
132	Ultrafast carrier transfer evidencing graphene electromagnetically enhanced ultrasensitive SERS in graphene/Ag-nanoparticles hybrid. Carbon, 2017, 122, 98-105.	10.3	40
133	Plasmon-exciton coupling of monolayer MoS2-Ag nanoparticles hybrids for surface catalytic reaction. Materials Today Energy, 2017, 5, 72-78.	4.7	169
134	Visualization of weak interactions between quantum dot and graphene in hybrid materials. Scientific Reports, 2017, 7, 417.	3.3	11
135	Vibronic quantized tunneling controlled photoinduced electron transfer in an organic solar cell subjected to an external electric field. Physical Chemistry Chemical Physics, 2017, 19, 16105-16112.	2.8	26
136	D–Aâ~π–A System: Light Harvesting, Charge Transfer, and Molecular Designing. Journal of Physical Chemistry C, 2017, 121, 12546-12561.	3.1	100
137	Photoactive layer based on T-shaped benzimidazole dyes used for solar cell: from photoelectric properties to molecular design. Scientific Reports, 2017, 7, 45688.	3.3	40
138	Surface-enhanced Raman scattering of pyrazine on Au ₅ Al ₅ bimetallic nanoclusters. RSC Advances, 2017, 7, 12170-12178.	3.6	8
139	Graphene, hexagonal boron nitride, and their heterostructures: properties and applications. RSC Advances, 2017, 7, 16801-16822.	3.6	500
140	Atomicâ€Levelâ€Designed Catalytically Active Palladium Atoms on Ultrathin Gold Nanowires. Advanced Materials, 2017, 29, 1604571.	21.0	52
141	Molecular Tilting Alignment on Ag@C Nanocubes Monitored by Temperature-Dependent Surface Enhanced Raman Scattering. Scientific Reports, 2017, 7, 12865.	3.3	8
142	Magnetics and spintronics on two-dimensional composite materials of graphene/hexagonal boron nitride. Materials Today Physics, 2017, 3, 93-117.	6.0	56
143	Ag nanoparticles-TiO2 film hybrid for plasmon-exciton co-driven surface catalytic reactions. Applied Materials Today, 2017, 9, 251-258.	4.3	65
144	Electrical properties and applications of graphene, hexagonal boron nitride (h-BN), and graphene/h-BN heterostructures. Materials Today Physics, 2017, 2, 6-34.	6.0	305

#	Article	IF	CITATIONS
145	Plasmon–exciton coâ€driven surface catalytic reaction in electrochemical G‧ERS. Journal of Raman Spectroscopy, 2017, 48, 1144-1147.	2.5	26
146	Fluorescence Resonance Energy Transfer of Monomer via Photoisomerization. ChemistrySelect, 2017, 2, 6446-6451.	1.5	2
147	Unified Treatment for Plasmon–Exciton Co-driven Reduction and Oxidation Reactions. Langmuir, 2017, 33, 12102-12107.	3.5	84
148	Low resistivity of graphene nanoribbons with zigzag-dominated edge fabricated by hydrogen plasma etching combined with Zn/HCl pretreatment. Applied Physics Letters, 2017, 111, 203102.	3.3	3
149	Electrooptical Synergy on Plasmon–Excitonâ€Codriven Surface Reduction Reactions. Advanced Materials Interfaces, 2017, 4, 1700869.	3.7	91
150	Optical, photonic and optoelectronic properties of graphene, h-BN and their hybrid materials. Nanophotonics, 2017, 6, 943-976.	6.0	78
151	Physical mechanism on exciton-plasmon coupling revealed by femtosecond pump-probe transient absorption spectroscopy. Materials Today Physics, 2017, 3, 33-40.	6.0	78
152	Tip-enhanced photoluminescence spectroscopy of monolayer MoS_2. Photonics Research, 2017, 5, 745.	7.0	33
153	Pt-Based Nanostructures for Observing Genuine SERS Spectra of p-Aminothiophenol (PATP) Molecules. Applied Sciences (Switzerland), 2017, 7, 953.	2.5	6
154	High-Vacuum Tip-Enhanced Raman Spectroscopy. , 2017, , 129-140.		0
155	Plasmonâ€driven catalysis in aqueous solutions probed by SERS spectroscopy. Journal of Raman Spectroscopy, 2016, 47, 877-883.	2.5	39
156	Farâ€Field Spectroscopy and Nearâ€Field Optical Imaging of Coupled Plasmon–Phonon Polaritons in 2D van der Waals Heterostructures. Advanced Materials, 2016, 28, 2931-2938.	21.0	77
157	High vacuum tip-enhanced Raman spectroscope based on a scanning tunneling microscope. Review of Scientific Instruments, 2016, 87, 033104.	1.3	86
158	How was the proton transfer process in bis-3, 6-(2- benzoxazolyl)-pyrocatechol, single or double proton transfer?. Scientific Reports, 2016, 6, 25568.	3.3	29
159	Facile Fabrication of Highâ€Density Subâ€1â€nm Gaps from Au Nanoparticle Monolayers as Reproducible SERS Substrates. Advanced Functional Materials, 2016, 26, 8137-8145.	14.9	143
160	Tip-Enhanced Raman Spectroscopy. Analytical Chemistry, 2016, 88, 9328-9346.	6.5	180
161	Orientation-and polarization-dependent optical properties of the single Ag nanowire/glass substrate system excited by the evanescent wave. Scientific Reports, 2016, 6, 25633.	3.3	13
162	Selective plasmon-driven catalysis for para-nitroaniline in aqueous environments. Scientific Reports, 2016, 6, 20458.	3.3	25

#	Article	IF	CITATIONS
163	A Nanoplasmonic Strategy for Precision in-situ Measurements of Tip-enhanced Raman and Fluorescence Spectroscopy. Scientific Reports, 2016, 6, 19558.	3.3	32
164	Theoretical Investigations of Optical Origins of Fluorescent Graphene Quantum Dots. Scientific Reports, 2016, 6, 24850.	3.3	64
165	Ultrafast Dynamics of Plasmon-Exciton Interaction of Ag Nanowire- Graphene Hybrids for Surface Catalytic Reactions. Scientific Reports, 2016, 6, 32724.	3.3	106
166	Photoinduced Electron Transfer in Organic Solar Cells. Chemical Record, 2016, 16, 734-753.	5.8	66
167	Surface plasmon-driven photocatalysis in ambient, aqueous and high-vacuum monitored by SERS and TERS. Journal of Photochemistry and Photobiology C: Photochemistry Reviews, 2016, 27, 100-112.	11.6	88
168	Propagating Surface Plasmon Polaritons: Towards Applications for Remoteâ€Excitation Surface Catalytic Reactions. Advanced Science, 2016, 3, 1500215.	11.2	106
169	Ascertaining Plasmonic Hot Electrons Generation from Plasmon Decay in Hybrid Plasmonic Modes. Plasmonics, 2016, 11, 909-915.	3.4	4
170	A plasmon-driven selective surface catalytic reaction revealed by surface-enhanced Raman scattering in an electrochemical environment. Scientific Reports, 2015, 5, 11920.	3.3	42
171	Formation of Enhanced Uniform Chiral Fields in Symmetric Dimer Nanostructures. Scientific Reports, 2015, 5, 17534.	3.3	66
172	Three Dimensional Hybrids of Vertical Graphene-nanosheet Sandwiched by Ag-nanoparticles for Enhanced Surface Selectively Catalytic Reactions. Scientific Reports, 2015, 5, 16019.	3.3	59
173	Photoinduced Charge Transport in a BHJ Solar Cell Controlled by an External Electric Field. Scientific Reports, 2015, 5, 13970.	3.3	33
174	Effect of aqueous and ambient atmospheric environments on plasmon-driven selective reduction reactions. Scientific Reports, 2015, 5, 10269.	3.3	22
175	Plasmon-driven reaction controlled by the number of graphene layers and localized surface plasmon distribution during optical excitation. Light: Science and Applications, 2015, 4, e342-e342.	16.6	178
176	Plasmon-driven sequential chemical reactions in an aqueous environment. Scientific Reports, 2015, 4, 5407.	3.3	51
177	Amplitude- and Phase-Resolved Nanospectral Imaging of Phonon Polaritons in Hexagonal Boron Nitride. ACS Photonics, 2015, 2, 790-796.	6.6	115
178	An in situ SERS study of substrate-dependent surface plasmon induced aromatic nitration. Journal of Materials Chemistry C, 2015, 3, 5285-5291.	5.5	23
179	Recent progress in the applications of graphene in surface-enhanced Raman scattering and plasmon-induced catalytic reactions. Journal of Materials Chemistry C, 2015, 3, 9024-9037.	5.5	113
180	Effect of Electric Field Gradient on Sub-nanometer Spatial Resolution of Tip-enhanced Raman Spectroscopy. Scientific Reports, 2015, 5, 9240.	3.3	83

#	Article	IF	CITATIONS
181	Nanoplasmonic waveguides: towards applications in integrated nanophotonic circuits. Light: Science and Applications, 2015, 4, e294-e294.	16.6	488
182	Insight into external electric field dependent photoinduced intermolecular charge transport in BHJ solar cell materials. Journal of Materials Chemistry C, 2015, 3, 4810-4819.	5.5	60
183	Near field plasmonic gradient effects on high vacuum tip-enhanced Raman spectroscopy. Physical Chemistry Chemical Physics, 2015, 17, 783-794.	2.8	41
184	Plasmon-driven surface catalysis in hybridized plasmonic gap modes. Scientific Reports, 2015, 4, 7087.	3.3	49
185	Nanowire-supported plasmonic waveguide for remote excitation of surface-enhanced Raman scattering. Light: Science and Applications, 2014, 3, e199-e199.	16.6	190
186	Plasmonic Gradient Effects on High Vacuum Tipâ€Enhanced Raman Spectroscopy. Advanced Optical Materials, 2014, 2, 74-80.	7.3	63
187	Tip-Enhanced Raman Spectroscopy: Plasmon-Driven Selective Reductions Revealed by Tip-Enhanced Raman Spectroscopy (Adv. Mater. Interfaces 5/2014). Advanced Materials Interfaces, 2014, 1, n/a-n/a.	3.7	1
188	Plasmonâ€Driven Selective Reductions Revealed by Tipâ€Enhanced Raman Spectroscopy. Advanced Materials Interfaces, 2014, 1, 1300125.	3.7	44
189	High-vacuum tip enhanced Raman spectroscopy. Frontiers of Physics, 2014, 9, 17-24.	5.0	14
190	Submonolayer-Pt-Coated Ultrathin Au Nanowires and Their Self-Organized Nanoporous Film: SERS and Catalysis Active Substrates for Operando SERS Monitoring of Catalytic Reactions. Journal of Physical Chemistry Letters, 2014, 5, 969-975.	4.6	59
191	Insight into vibration mode-resolved plasmon enhanced Raman optical activity. Journal of Colloid and Interface Science, 2014, 415, 165-168.	9.4	2
192	Bioorganic dye-sensitized solar cell of carotenoid–pheophytin a–TiO ₂ . RSC Advances, 2014, 4, 63016-63024.	3.6	15
193	Molecular resonant dissociation of surface-adsorbed molecules by plasmonic nanoscissors. Nanoscale, 2014, 6, 4903-4908.	5.6	43
194	Probing Local Strain at MX ₂ –Metal Boundaries with Surface Plasmon-Enhanced Raman Scattering. Nano Letters, 2014, 14, 5329-5334.	9.1	118
195	Elastic Properties of Chemical-Vapor-Deposited Monolayer MoS ₂ , WS ₂ , and Their Bilayer Heterostructures. Nano Letters, 2014, 14, 5097-5103.	9.1	512
196	Ultrafast charge transfer in atomically thin MoS2/WS2 heterostructures. Nature Nanotechnology, 2014, 9, 682-686.	31.5	1,838
197	Synergistic Modulation of Surface Interaction to Assemble Metal Nanoparticles into Twoâ€Dimensional Arrays with Tunable Plasmonic Properties. Small, 2014, 10, 609-616.	10.0	51
198	Visualized method of chemical enhancement mechanism on SERS and TERS. Journal of Raman Spectroscopy, 2014, 45, 533-540.	2.5	107

#	Article	IF	CITATIONS
199	Plasmon-driven dimerization via S-S chemical bond in an aqueous environment. Scientific Reports, 2014, 4, 7221.	3.3	19
200	Tip-Enhanced Ultrasensitive Stokes and Anti-Stokes Raman Spectroscopy in High Vacuum. Plasmonics, 2013, 8, 523-527.	3.4	15
201	Accurate double manyâ€body expansion potential energy surface by extrapolation to the complete basis set limit and dynamics calculations for ground state of NH ₂ . Journal of Computational Chemistry, 2013, 34, 1686-1696.	3.3	32
202	External Electric Field-Dependent Photoinduced Charge Transfer in a Donor–Acceptor System for an Organic Solar Cell. Journal of Physical Chemistry C, 2013, 117, 15879-15889.	3.1	129
203	Nanoparticle Catalysis by Surface Plasmon. , 2013, , 473-487.		2
204	Remote-Excitation Time-Dependent Surface Catalysis Reaction Using Plasmonic Waveguide on Sites of Single-Crystalline Crossed Nanowires. Plasmonics, 2013, 8, 249-254.	3.4	17
205	Interlayer catalytic exfoliation realizing scalable production of large-size pristine few-layer graphene. Scientific Reports, 2013, 3, 1134.	3.3	83
206	Excitation of Surface Plasmon Resonance in Composite Structures Based on Single-Layer Superaligned Carbon Nanotube Films. Journal of Physical Chemistry C, 2013, 117, 23190-23197.	3.1	12
207	High-Density Three-Dimension Graphene Macroscopic Objects for High-Capacity Removal of Heavy Metal Ions. Scientific Reports, 2013, 3, 2125.	3.3	129
208	Electric field gradient quadrupole Raman modes observed in plasmon-driven catalytic reactions revealed by HV-TERS. Nanoscale, 2013, 5, 4151.	5.6	54
209	Activated vibrational modes and Fermi resonance in tip-enhanced Raman spectroscopy. Physical Review E, 2013, 87, 020401.	2.1	78
210	Insights into the nature of plasmon-driven catalytic reactions revealed by HV-TERS. Nanoscale, 2013, 5, 3249.	5.6	84
211	Electronic transport properties of graphene nanoribbon arrays fabricated by unzipping aligned nanotubes. Physical Review B, 2013, 87, .	3.2	21
212	Tipâ€Enhanced Resonance Couplings Revealed by High Vacuum Tipâ€Enhanced Raman Spectroscopy. Advanced Optical Materials, 2013, 1, 449-455.	7.3	39
213	Accurate <i>ab initio</i> -based adiabatic global potential energy surface for the 22 <i>A</i> ″ state of NH2 by extrapolation to the complete basis set limit. Journal of Chemical Physics, 2013, 139, 154305.	3.0	29
214	Bringing java's wild native world under control. ACM Transactions on Information and System Security, 2013, 16, 1-28.	4.5	14
215	Remotely excited Raman optical activity using chiral plasmon propagation in Ag nanowires. Light: Science and Applications, 2013, 2, e112-e112.	16.6	185
216	Plasmonic Scissors for Molecular Design. Chemistry - A European Journal, 2013, 19, 14958-14962.	3.3	89

#	Article	IF	CITATIONS
217	In-situ plasmon-driven chemical reactions revealed by high vacuum tip-enhanced Raman spectroscopy. Scientific Reports, 2012, 2, 647.	3.3	254
218	Nonlinear resonances in electrochemical SERS of SCNâ [~] ', rotation-resolved Raman and anti-Stokes Raman of SCNâ [~] ' in HV-TERS. RSC Advances, 2012, 2, 12160.	3.6	2
219	Ascertaining genuine SERS spectra of p-aminothiophenol. RSC Advances, 2012, 2, 8289.	3.6	33
220	Visualizations of charge transfer for the model of poly(3,4-alkylenedioxythiophene)s in neutral and various oxidation states. RSC Advances, 2012, 2, 12983.	3.6	8
221	Theoretical study on polyaniline gas sensors: Examinations of response mechanism for alcohol. Synthetic Metals, 2012, 162, 862-867.	3.9	27
222	A Novel Application of Plasmonics: Plasmonâ€Driven Surfaceâ€Catalyzed Reactions. Small, 2012, 8, 2777-2786.	10.0	409
223	<i>Ab initio</i> -based double many-body expansion potential energy surface for the first excited triplet state of the ammonia molecule. Journal of Chemical Physics, 2012, 136, 194705.	3.0	25
224	Selective reduction of nitroaromatic compounds on silver nanoparticles by visible light. Journal of Raman Spectroscopy, 2012, 43, 1024-1028.	2.5	7
225	Layerâ€Controlled and Waferâ€Scale Synthesis of Uniform and Highâ€Quality Graphene Films on a Polycrystalline Nickel Catalyst. Advanced Functional Materials, 2012, 22, 3153-3159.	14.9	93
226	Can information of chemical reaction propagate with plasmonic waveguide and be detected at remote terminal of nanowire?. Nanoscale, 2011, 3, 4114.	5.6	28
227	Deep ultraviolet tip-enhanced Raman scattering. Chemical Communications, 2011, 47, 9131.	4.1	40
228	Substrate-, Wavelength-, and Time-Dependent Plasmon-Assisted Surface Catalysis Reaction of 4-Nitrobenzenethiol Dimerizing to <i>p</i> , <i>p</i> ′-Dimercaptoazobenzene on Au, Ag, and Cu Films. Langmuir, 2011, 27, 10677-10682.	3.5	223
229	Remote Excitation of Surface-Enhanced Raman Scattering on Single Au Nanowire with Quasi-Spherical Termini. Journal of Physical Chemistry C, 2011, 115, 3558-3561.	3.1	44
230	Fabrication of a Au Nanoporous Film by Self-Organization of Networked Ultrathin Nanowires and Its Application as a Surface-Enhanced Raman Scattering Substrate for Single-Molecule Detection. Analytical Chemistry, 2011, 83, 9131-9137.	6.5	52
231	Theoretical Characterization of the PC ₆₀ BM:PDDTT Model for an Organic Solar Cell. Journal of Physical Chemistry C, 2011, 115, 21865-21873.	3.1	213
232	The pH-Controlled Plasmon-Assisted Surface Photocatalysis Reaction of 4-Aminothiophenol to <i>p</i> , <i>p</i> ′-Dimercaptoazobenzene on Au, Ag, and Cu Colloids. Journal of Physical Chemistry C, 2011, 115, 9629-9636.	3.1	149
233	Reduced Graphene Oxide Electrically Contacted Graphene Sensor for Highly Sensitive Nitric Oxide Detection. ACS Nano, 2011, 5, 6955-6961.	14.6	367
234	Synthesis of hollow polypyrrole-platinum complex spheres and their successful application as a catalyst for decomposition of hydrogen peroxide. Kinetics and Catalysis, 2011, 52, 716-722.	1.0	1

#	Article	IF	CITATIONS
235	Electrical and Raman properties of p-type and n-type modified graphene by inorganic quantum dot and organic molecule modification. Science China: Physics, Mechanics and Astronomy, 2011, 54, 416-419.	5.1	14
236	Remote Excitation Surface Plasmon and Consequent Enhancement of Surface-Enhanced Raman Scattering Using Evanescent Wave Propagating in Quasi-One-Dimensional MoO3 Ribbon Dielectric Waveguide. Plasmonics, 2011, 6, 189-193.	3.4	24
237	Remote Excitation Polarization-Dependent Surface Photochemical Reaction by Plasmonic Waveguide. Plasmonics, 2011, 6, 681-687.	3.4	45
238	Is 4â€nitrobenzenethiol converted to <i>p</i> , <i>p</i> ′â€dimercaptoazobenzene or 4â€aminothiophenol by surface photochemistry reaction?. Journal of Raman Spectroscopy, 2011, 42, 1205-1206.	2.5	119
239	Quasi-one dimensional Er3+–Yb3+ codoped single-crystal MoO3 ribbons: Synthesis, characterization and up-conversion luminescence. Optics Communications, 2011, 284, 2528-2531.	2.1	9
240	Local and Remote Chargeâ€Transferâ€Enhanced Raman Scattering on Oneâ€Dimensional Transitionâ€Metal Oxides. Chemistry - an Asian Journal, 2010, 5, 1824-1829.	3.3	42
241	Aqueousâ€Processable Noncovalent Chemically Converted Graphene–Quantum Dot Composites for Flexible and Transparent Optoelectronic Films. Advanced Materials, 2010, 22, 638-642.	21.0	288
242	Adjustment and control of SERS activity of metal substrates by pressure. Journal of Raman Spectroscopy, 2010, 41, 398-405.	2.5	10
243	Experimental and theoretical evidence for the chemical mechanism in SERRS of rhodamine 6G adsorbed on colloidal silver excited at 1064 nm. Journal of Raman Spectroscopy, 2010, 41, 719-720.	2.5	10
244	A one-step facile synthesis of Ag–Ni core–shell nanoparticles in water-in-oil microemulsions. Colloids and Surfaces A: Physicochemical and Engineering Aspects, 2010, 367, 96-101.	4.7	35
245	Ascertaining p, pʹ-dimercaptoazobenzene Produced from p-aminothiophenol by Selective Catalytic Coupling Reaction on Silver Nanoparticles. , 2010, , .		3
246	Ascertaining <i>p</i> , <i>p</i> ′-Dimercaptoazobenzene Produced from <i>p</i> -Aminothiophenol by Selective Catalytic Coupling Reaction on Silver Nanoparticles. Langmuir, 2010, 26, 7737-7746.	3.5	343
247	Directed Calcium Chloride Coalescence Method for Preparation of Silver Nanocubes. Applied Spectroscopy, 2010, 64, 867-870.	2.2	1
248	Can <i>p</i> , <i>p</i> ′-Dimercaptoazobisbenzene Be Produced from <i>p</i> -Aminothiophenol by Surface Photochemistry Reaction in the Junctions of a Ag Nanoparticleâ^'Moleculeâ^'Ag (or Au) Film?. Journal of Physical Chemistry C, 2010, 114, 18263-18269.	3.1	114
249	Direct Visualization of the Chemical Mechanism in SERRS of 4â€Aminothiophenol/Metal Complexes and Metal/4â€Aminothiophenol/Metal Junctions. ChemPhysChem, 2009, 10, 392-399.	2.1	62
250	Direct visual evidence for the chemical mechanism of surfaceâ€enhanced resonance Raman scattering via charge transfer. Journal of Raman Spectroscopy, 2009, 40, 137-143.	2.5	79
251	Direct visual evidence for the chemical mechanism of surfaceâ€enhanced resonance Raman scattering via charge transfer: (II) Bindingâ€site and quantumâ€size effects. Journal of Raman Spectroscopy, 2009, 40, 1172-1177.	2.5	28
252	Direct visual evidence for chemical mechanisms of SERRS via charge transfer in Au ₂₀ –pyrazine–Au ₂₀ junction. Journal of Raman Spectroscopy, 2009, 40, 1942-1948.	2.5	21

#	Article	IF	CITATIONS
253	DFT study of adsorption site effect on surface-enhanced Raman scattering of neutral and charged pyridine–Ag4 complexes. Spectrochimica Acta - Part A: Molecular and Biomolecular Spectroscopy, 2009, 73, 382-387.	3.9	46
254	Self-assembled dynamics of silver nanoparticles and self-assembled dynamics of 1,4-benzenedithiol adsorbed on silver nanoparticles: Surface-enhanced Raman scattering study. Spectrochimica Acta - Part A: Molecular and Biomolecular Spectroscopy, 2009, 74, 509-514.	3.9	10
255	Photoexcitation mechanisms of centrosymmetric and asymmetric fluorene derivatives in two-photon absorption. Chemical Physics, 2009, 359, 166-172.	1.9	14
256	Near- and Deep-Ultraviolet Resonance Raman Spectroscopy of Pyrazineâ^'Al ₄ Complex and Al ₃ â^'Pyrazineâ^'Al ₃ Junction. Journal of Physical Chemistry C, 2009, 113, 19328-19334.	3.1	21
257	Chemical and electromagnetic mechanisms of tip-enhanced Raman scattering. Physical Chemistry Chemical Physics, 2009, 11, 9412.	2.8	61
258	Surface enhanced Raman scattering of pyridine adsorbed on Au@Pd core/shell nanoparticles. Journal of Chemical Physics, 2009, 130, 234705.	3.0	51
259	Excited state properties of neutral and charged terâ€fluorene with and without a ketoâ€defect. Physica Status Solidi (B): Basic Research, 2008, 245, 849-853.	1.5	14
260	Chemical mechanism of surfaceâ€enhanced resonance Raman scattering via charge transfer in pyridine–Ag ₂ complex. Journal of Raman Spectroscopy, 2008, 39, 402-408.	2.5	77
261	Theoretical study on SERRS of rhodamine 6G adsorbed on Ag ₂ cluster: chemical mechanism via intermolecular or intramolecular charge transfer. Journal of Raman Spectroscopy, 2008, 39, 1170-1177.	2.5	23
262	Photoinduced Intramolecular Charge Transfer and S ₂ Fluorescence in Thiopheneâ€ï€â€Conjugated Donor–Acceptor Systems: Experimental and TDDFT Studies. Chemistry - A European Journal, 2008, 14, 6935-6947.	3.3	203
263	Spinâ€orbit <i>Ab initio</i> investigation of the photodissociation of dibromomethane in the gas and solution phases. Journal of Computational Chemistry, 2008, 29, 2513-2519.	3.3	7
264	Photoinduced intramolecular charge-transfer state in thiophene-ï€-conjugated donor–acceptor molecules. Journal of Molecular Structure, 2008, 876, 102-109.	3.6	72
265	Visualizations of transition dipoles, charge transfer, and electron-hole coherence on electronic state transitions between excited states for two-photon absorption. Journal of Chemical Physics, 2008, 128, 064106.	3.0	68
266	Microwave-assisted synthesis of sensitive silver substrate for surface-enhanced Raman scattering spectroscopy. Journal of Chemical Physics, 2008, 129, 134703.	3.0	26
267	Do coupling exciton and oscillation of electron-hole pair exist in neutral and charged π-dimeric quinquethiophenes?. Journal of Chemical Physics, 2007, 127, 084706.	3.0	29
268	Direct Visual Evidence for Quinoidal Charge Delocalization in Poly- <i>p</i> -phenylene Cation Radical. Journal of Physical Chemistry B, 2007, 111, 13266-13270.	2.6	34
269	S1 and S2 Excited States of Gas-Phase Schiff-Base Retinal Chromophores:  A Time-Dependent Density Functional Theoretical Investigation. Journal of Physical Chemistry A, 2007, 111, 2946-2950.	2.5	34
270	Two-photon photophysical properties of tri-9-anthrylborane. Chemical Physics Letters, 2007, 436, 280-286.	2.6	25

#	Article	IF	CITATIONS
271	Spectroscopic and theoretical studies on the photophysical properties of dichlorotriazine derivatives. Chemical Physics Letters, 2007, 444, 297-303.	2.6	4
272	Photoabsorption of green and red fluorescent protein chromophore anions in vacuo. Biophysical Chemistry, 2007, 129, 218-223.	2.8	35
273	The charge transfer mechanism and spectral properties of a near-infrared heptamethine cyanine dye in alcoholic and aprotic solvents. Journal of Photochemistry and Photobiology A: Chemistry, 2007, 187, 305-310.	3.9	86
274	Control of Emission by Intermolecular Fluorescence Resonance Energy Transfer and Intermolecular Charge Transfer. Journal of Physical Chemistry A, 2006, 110, 6324-6328.	2.5	52
275	Excited state properties of the chromophore of the asFP595 chromoprotein: 2D and 3D theoretical analyses. International Journal of Quantum Chemistry, 2006, 106, 1020-1026.	2.0	28
276	Comparison of the electronic structure of PPV and its derivative DIOXA-PPV. Chemical Physics, 2006, 327, 474-484.	1.9	96
277	Excited state properties of novel p- and n-type organic semiconductors with an anthracene unit. Chemical Physics, 2006, 320, 155-163.	1.9	31
278	Control of structure and photophysical properties by protonation and subsequent intramolecular hydrogen bonding. Journal of Chemical Physics, 2006, 124, 054903.	3.0	118
279	CHARGE AND ENERGY TRANSFER IN BINAPHTHALENE MOLECULE WITH TWO SPIROPYRAN UNITS USED FOR CHIRAL MOLECULAR SWITCHES AND LOGIC GATES. Journal of Theoretical and Computational Chemistry, 2006, 05, 163-174.	1.8	8
280	Excited state properties of acceptor-substitute carotenoids: 2D and 3D real-space analysis. Chemical Physics Letters, 2005, 401, 558-564.	2.6	28
281	Charge transfer state induced from locally excited state by polar solvent. Chemical Physics Letters, 2005, 408, 128-133.	2.6	26
282	Intermolecular charge and energy transfer in neurosporene and chlorophyll a derivative complex. Chemical Physics Letters, 2005, 412, 425-429.	2.6	21
283	Intramolecular charge transfer and locally excited states of the fullerene-linked quarter-thiophenes dyad. Chemical Physics Letters, 2005, 413, 110-117.	2.6	32
284	Intramolecular charge transfer in the porphyrin–oligothiophene–fullerene triad. Chemical Physics Letters, 2005, 416, 94-99.	2.6	29
285	Optical properties of low band gap alternating copolyfluorenes for photovoltaic devices. Journal of Chemical Physics, 2005, 123, 204718.	3.0	80
286	Collisional quantum interference on rotational energy transfer in Na2 (A1Σu+,v=8â^¼b3Î0u,v=14)–Na system. Chemical Physics Letters, 2004, 386, 430-436.	2.6	8
287	Quantum interference in collision-induced energy transfer for CO (A1Î,v=0/e3Σâ~',v=1)–HCl (X1Σ) system studied by OODR-MPI spectroscopy. Chemical Physics Letters, 2004, 388, 306-311.	2.6	7
288	Collision-induced rotational energy transfer of CO (A1î,v=3) with He, Ne and Ar: (II) theoretical interpretation of the experiment. Chemical Physics Letters, 2003, 371, 342-348.	2.6	10

#	Article	IF	CITATIONS
289	ĥ-Related quantum interference of Î-state diatomic on collision-induced rotational energy transfer. Chemical Physics Letters, 2003, 374, 20-27.	2.6	9
290	Rotational energy transfer on CO (e3Σⴒ,v=1) collision with He: interpretation of the propensity rules. Chemical Physics Letters, 2003, 378, 148-154.	2.6	0
291	Collisional quantum interference on rotational energy transfer in Na2 (A 1Σu+, v = 8 â^¼â€‰b 3Î0 system. Physical Chemistry Chemical Physics, 2003, 5, 1570-1574.	u,v =ä 2.8	14)– 4
292	Further theoretical study of collisional quantum interference on rotational energy transfer in an atom–diatom system. Physical Chemistry Chemical Physics, 2002, 4, 5123-5127.	2.8	10
293	Collisional quantum interference on rotational energy transfer: (II) in a polar diatom–diatom system. Chemical Physics Letters, 2002, 361, 8-14.	2.6	10
294	2+1+1 two-color REMPI study of the E1Î(ν=1)â†Đ1Δ(ν=10)â†X1Σ+(ν=0) transition in CO: influence of the a predissociation in the CO E1Î(ν=1) state at j=9 and 10. Chemical Physics Letters, 2002, 359, 520-523.	ccidental	2
295	Collision-induced rotational energy transfer of CO (A1Î,v=3) with He, Ne and Ar: experiment via two-color 2+1+1 REMPI technique. Chemical Physics Letters, 2002, 365, 244-250.	2.6	12
296	Collisional quantum interference effect on rotational energy transfer in an atom–diatom system. Chemical Physics Letters, 2001, 339, 413-420.	2.6	18
297	Collisional quantum interference on rotational energy transfer: physical interpretation of the interference angle. Chemical Physics, 2001, 274, 175-186.	1.9	15
298	A metal plasma source ion implantation and deposition system. Review of Scientific Instruments, 1999, 70, 1816-1820.	1.3	0
299	Surface-Enhanced Coherent Anti-Stokes Raman Scattering Based on Coupled Nanohole-Slit Arrays. Physical Chemistry Chemical Physics, 0, , .	2.8	1